INTERNATIONAL JOURNAL OF COMPUTERS COMMUNICATIONS & CONTROL
Online ISSN 1841-9844, ISSN-L 1841-9836, Volume: 21, Issue: 5, Month: October, Year: 2026
Article Number: 7202, https://doi.org/10.15837/ijccc.2026.5.7202

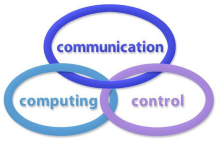

CCC Publications

Sequential Feature Selection and Adaptive Ensemble Classification for Parkinson's Disease Detection

Zhimin Zheng, Kaidi Gong, Chen Gong, Lifang Zhang, Lin Meng, Feng He*

Zhimin Zheng
Academy of Medical Engineering and Translational Medicine, Tianjin University, Tianjin, China, 300072
China Mobile Research Institute, Beijing, China, 100053
zhengzhimin@chinamobile.com

Kaidi Gong
China Mobile Research Institute, Beijing, China, 100053
gongkaidi@chinamobile.com

Chen Gong
China Mobile Research Institute, Beijing, China, 100053
gongchenyjy@chinamobile.com

Lifang Zhang
The Eighth People's Hospital of Longgang District, Shenzhen, China, 518116
The Affiliated Brain Hospital of Guangzhou Medical University, Guangzhou, China, 510170
zhanglifang1976111@gzhmu.edu.cn

Lin Meng
Academy of Medical Engineering and Translational Medicine, Tianjin University, Tianjin, China, 300072
linmeng@tju.edu.cn

Feng He
Academy of Medical Engineering and Translational Medicine, Tianjin University, Tianjin, China, 300072
*Corresponding author: heaven@tju.edu.cn

Abstract

Parkinson's Disease (PD) significantly affects motor functions, with gait disturbances being a signal symptom. This study leverages biomedical information fusion to enhance PD diagnosis through gait analysis. Using a 6-axis inertial measurement unit (IMU) mounted on insoles, we collected a comprehensive dataset comprising over 2,000 samples and 164 gait features from PD patients and healthy controls. A novel sequential feature selection strategy was developed, reducing redundancy and identifying 41 critical gait metrics, enabling efficient and interpretable analysis. An adaptive voting ensemble model was proposed, effectively addressing patient heterogeneity and achieving superior predictive performance with an AUC of 0.9055. This method has the potential to optimize wearable systems to facilitate real-time monitoring and early interventions for PD.

Keywords: Parkinson's Disease, gait analysis, feature selection, ensemble machine learning, wearable devices, biomedical information fusion.

1 Introduction

Parkinson's Disease (PD) is the second most common neurodegenerative disorder globally, following Alzheimer's disease [10]. Characterized by progressive symptoms such as tremors, rigidity, and bradykinesia, PD significantly diminishes the quality of life for those affected. With an aging global

population, the prevalence of PD is anticipated to increase markedly, posing substantial challenges for healthcare systems. In China, the number of individuals diagnosed with PD is projected to reach 5 million by 2030, underscoring the urgent need for improved disease management strategies [4].

Given this rising prevalence, early diagnosis has become increasingly critical in mitigating the progression of PD. Timely medical intervention can substantially improve patient outcomes. However, current diagnostic approaches rely heavily on clinical presentations, alongside ancillary tests like computed tomography (CT) and magnetic resonance imaging (MRI) to rule out other conditions that might cause similar symptoms. However, these methods lack sensitivity for early-stage detection and specificity for PD diagnosis, leading to frequent misdiagnosis and delayed identification. As a result, delays in diagnosis often lead to symptom worsening, greater movement impairments, and reduced treatment effectiveness. This highlights the need to develop advanced diagnostic technologies that can reliably detect PD more accurately and sensitively.

Abnormal posture and gait are among the most apparent symptoms in the early stages of PD [23]. Patients typically exhibit gait slowing, shortened stride length, and reduced arm swing amplitude [8, 21]. Additionally, there is a reduction in the range of motion of the hip, knee, and ankle joints, especially during the late stance phase of the gait cycle [6]. These changes lead to increased gait asymmetry and variability, resulting in distinctive abnormal gait patterns. As the disease progresses to its mid- and later stages, gait disturbances such as freezing of gait (FOG), gait hesitation, and hurried gait become more pronounced[23], significantly impairing motor function. These abnormalities severely affect the patient's ability to perform daily activities and increase the risk of falls.

Given the critical role of gait in PD progression, gait assessment has become an essential component of disease management. By analyzing gait characteristics, it is possible to monitor disease progression and assess treatment efficacy. Gait assessment methods can be broadly categorized into subjective and objective measurements. Subjective measurements involve clinicians or healthcare professionals visually observing and scoring the patient's gait using standardized rating scales, such as the gait section of the Unified Parkinson's Disease Rating Scale (UPDRS) and its modified versions [16, 19], the Hoehn-Yahr (H&Y) staging scale [3], and the Freezing of Gait Questionnaire (FOG-Q) [12]. While these methods are simple, cost-effective, and quick to administer in clinical settings, they are subject to observer bias, reducing the reliability and consistency of results. Moreover, subjective measurements cannot provide precise quantitative data and may miss subtle changes in gait, making them less effective for early detection and monitoring fine variations in disease progression.

Objective measurement methods, on the other hand, use specialized equipment, such as optical motion capture systems (e.g., VICON) [22], inertial measurement units (IMUs) [17], and pressure-sensitive walkway [15], to capture and analyze detailed gait parameters. These methods offer greater precision and are capable of detecting subtle gait abnormalities. However, these devices are typically limited to hospital or laboratory settings due to their complexity and high cost, making them impractical for home use. This limits the frequency of gait assessments and hinders their application for routine monitoring. Furthermore, as PD is a neurological disorder, the "observer effect" may influence gait patterns, as patients may alter their natural gait under the scrutiny of healthcare professionals. Additionally, certain symptoms, such as FOG, are intermittent and sudden in onset, ans thus may not be captured within the limited time available during outpatient clinic visits.

To address these gaps, this study focuses on home-based intelligent PD detection using simple yet effective sensors. Leveraging a large-scale Chinese gait dataset comprising over 2,000 samples and 164 gait features collected via a 6-axis IMU embedded in insoles, we propose a more generalizable framework for early PD detection. Specifically, our contributions are as follows:

- By utilizing a gait dataset of over 2,000 samples, we address the limitations of existing studies that lack proofs on large-scale data from lower-limb or foot-mounted sensors. This approach provides more consistent gait data compared to smartphone-based methods, leading to superior performance.

- We introduce a novel sequential feature selection strategy applied to 164 gait features, offering more comprehensive insights into key gait characteristics associated with PD.

- We develop an adaptive voting ensemble model that effectively captures the gait heterogeneity, achieving enhanced predictive accuracy for distinguishing PD patients from healthy controls.

2 Related Works

As the improvement of sensors and information techniques, the combination of advanced sensor technologies and machine learning approaches has significantly improved gait analysis, enabling more accurate assessment of PD.

2.1 Gait Analysis and Gait Parameters

The gait cycle of a healthy adult is a repetitive, cyclical process lasting about 1 to 1.32 seconds [9]. The gait cycle is often broadly divided into stance and swing phases. By further subdividing the stance phase, it can be partitioned into four distinct phases: loading, flatfoot, push-off, and swing.[14]. These phases can be identified by key gait events including heel strike, heel off, foot flat, and toe off.

Human gait evaluation involves assessing postural control, balance, and coordination. Gait parameters are calculated after estimating the global posture direction and detecting gait events. These parameters can be classified into three categories: spatio-temporal, kinematic, and dynamic.

Spatio-temporal parameters—such as stride length, cadence, step width, and stance/swing duration—are critical for assessing gait and are particularly sensitive to PD[32]. Studies have shown that slowed gait speed, reduced stride length, increased cadence, and higher double support ratios are key spatiotemporal indicators of PD [11, 24].

Kinematic parameters, including joint angles, joint range of motion (ROM), and limb velocity, offer important insights into PD-related gait abnormalities. For instance, Parkinson's patients often experience significantly reduced ROM in the hip, knee, and ankle joints, which leads to altered gait patterns [29].

Dynamic parameters, such as foot pressure and ground reaction force (GRF), reflect the biomechanical aspects of gait and are often used for assessing PD severity. Vertical GRF, in particular, is a key marker for distinguishing PD patients from healthy individuals [31].

Despite the growing body of research, many studies focus on small gait feature sets or raw series data from the sensors, with limited efforts to analyze a wide range of gait features comprehensively and interpretably. Our work aims to fill this gap by offering a more holistic view of the gait parameters involved in PD detection.

2.2 Machine Learning in PD Gait Analysis

Recent advances in sensor technology have facilitated detailed gait data collection and laid the foundation for applying data-driven techniques to analyze gait and detect PD abnormalities. Various machine learning or deep learning algorithms, such as support vector machines (SVM), random forests, and convolutional neural networks, have been applied to PD gait analysis, tackling challenges such as disease staging [2, 18], FOG detection [26], and fall risk prediction [28].

Several studies have demonstrated the effectiveness of ML in PD diagnosis, with high classification accuracy reported using small datasets. For example, Rehman et al. [24] achieved 97.1% accuracy using random forest and temporal/spatial gait features from the GAITRite system, while Park et al. [20] combined temporal, spatial, and kinematic data with Random Forest to achieve 98.1% accuracy. Caramia et al. [5] achieved 96% accuracy with a soft-voting ensemble model based on ROM features. These results highlight the potential of ML models to detect PD, but the studies are often limited by small sample sizes and the use of only a few gait features.

There has been a push towards larger-scale studies, such as the work by Zhang et al. [33], which used data from over 2,000 healthy individuals and 656 PD patients. This study applied deep convolutional neural networks (DCNN) to continuous data from smartphone accelerometers, achieving an AUC score of 0.87. However, large-scale studies using lower-limb or foot data remain scarce. Our study addresses this gap by focusing on a broader range of derived gait characteristics and leveraging large-scale data to improve classification accuracy.

3 Materials and Methods

3.1 Gait Dataset Collected Using a Simplified IMU Setup

In collaboration with Tianjin Huanhu Hospital (TJHH) and the Neurology Hospital of Guangzhou Medical University (GZHBH-GZHMU), we systematically collected gait data from both Parkinson's disease (PD) patients and healthy volunteers. Participants wore only a pair of IMU sensors [1], placed at the bottom of the insole (Figure 1a). This sensor setup ensured accurate and stable data collection while maintaining portability and comfort. Operating at a sampling rate of 100Hz, the IMU captured six-dimensional data, including acceleration and angular velocity along the x, y, and z axes.

During the gait assessment, participants performed the walk straight and turn (WST) test [16], which aligns with item 3.10 "Gait" from the MDS-UPDRS scale [16]. The protocol involved starting from a standing position, walking a straight 10-meter path, executing a 180-degree turn, and returning to the starting point (illustrated in Figure 1b). Participants were instructed to perform the test in a smooth, continuous manner to simulate natural walking conditions. Clinically, the WST test enables clinicians to evaluate several aspects of the participant's gait, including stride length, walking speed, foot clearance, heel strike mechanics, turning ability, and the occurrence of FOG.

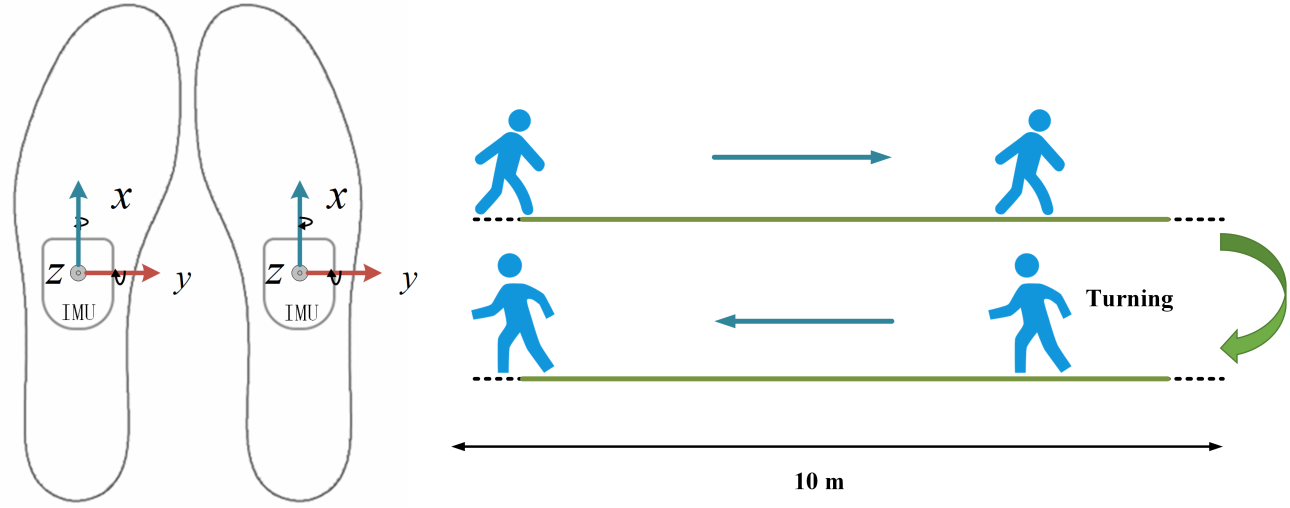

(a) IMU used for data collection.

(b) WST walking experiment paradigm.

Figure 1: Experimental Setup for Gait Data Collection.

Using the device's built-in data preprocessing and attitude calculation algorithms, we obtained 164 distinct gait parameters (See Table 6-10 in Appendix A) from the raw acceleration and angular velocity data. These parameters encompass temporal features (e.g., gait cycle and phase durations), spatial features (e.g., step length and width), and kinematic features (e.g., angular velocity changes relative to the ground). These comprehensive metrics offer a detailed understanding of gait characteristics and support the identification of health conditions associated with gait abnormalities.

The final dataset includes 207 PD patients and 2,186 healthy controls. The patient cohort comprised individuals with mild-to-moderate symptoms who were still capable of walking independently, allowing our study to specifically target a population where gait analysis can serve as a key tool for early-to-mid stage screening. Detailed information of the dataset is provided in Table 1. 70% of the data was randomly selected for training, while the remaining 30% was used for testing.

3.2 Overview of Methodology

In addressing the classification of disease populations, two primary challenges must be addressed. Firstly, the 164 gait parameters extracted in this study, result in high-dimension problems. Not all

[1]Dynamic Gait & Posture Analysis System, Right Gait & Posture 4.0, Shenzhen Xingzheng Technology Co., Ltd.

Table 1: Demographic characteristics of PD and HC groups.

	PD	HC
Count	207	2168
Gender ratio (M/F)	119/88	275/1893
Average age (years)	60	34
Average height (cm)	164	163
Average weight (kg)	64	57

features are relevant for every patient, and redundancy is inherently present. Secondly, the heterogeneity of the population complicates the classification process, as distinct patient subgroups may require tailored classification strategies.

To overcome these challenges, we employed a sequential feature selection strategy. The first stage involved preliminary feature selection using filtering methods to reduce computational complexity. Subsequently, we addressed the class imbalance by adopting synthetic minority oversampling technique (SMOTE). Following this, the second stage employed integrated model-driven feature selection combined with coarse-to-fine threshold optimization to enhance predictive performance. After feature selection was complete, an ensemble learning model with adaptive hyperparameter optimization was developed for PD detection, effectively combining the strengths of multiple classifiers to improve diagnostic accuracy. Figure 2 displays the overall methodology.

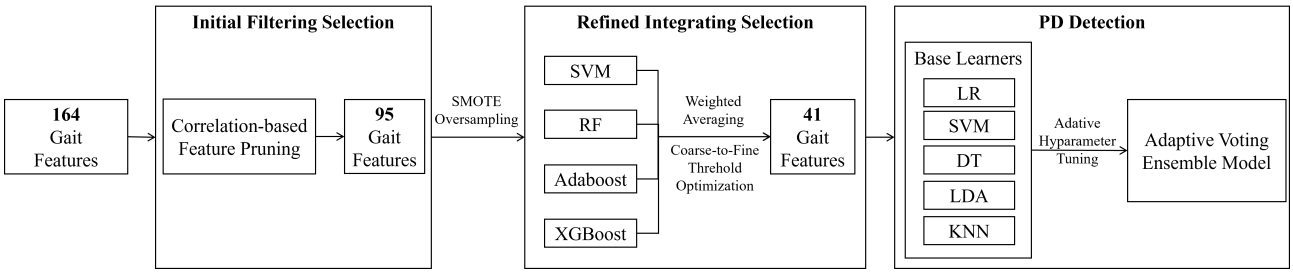

Figure 2: Overview of the methodology.

3.3 Sequential Feature Selection Strategy

We employed a two-stage sequential feature selection method to optimize gait data for PD assessment. The initial stage involved a filter-based backward elimination method: we iteratively identified the most highly correlated feature pair and removed the feature with the higher average correlation to the remaining variables. After this step, SMOTE oversampling was applied to adress the class imbalance problem. Subsequently, the second stage refined this set by integrating feature importance scores from multiple models and optimizing the corresponding importance threshold. This approach enhanced model generalizability and interpretability.

3.3.1 Preliminary Feature Selection through Filtering Methods

To optimize the elimination of redundant features, we employed a backward, correlation-based feature pruning process. The process began by computing the correlation matrix for all variables and identifying the pair with the highest correlation. For each identified pair, the average correlation of each variable with the others was calculated. The variable with the higher average correlation was then removed, and this process was repeated until all correlations fall below a specified threshold of 0.6. This method reduced redundancy in the feature set, enhancing computational efficiency and minimizing the risk of overfitting.

Table 2: Hyperparameters for adaptive fine-tuning.

Base Learner	Hyperparameters
SVM	C, gamma, kernel
DT	max_depth
LR	C
LDA	-
KNN	n_neighbors

3.3.2 Refined Feature Selection through Integrated Model-driven Methods with Coarse-to-Fine Threshold Optimization

Building on the features selected through preliminary filtering methods, feature selection was further refined by training and integrating four machine learning models: SVM, random forests, adaptive boosting (AdaBoost), and extreme gradient boosting machine (XGBoost). The objective was to derive feature importance scores from different models, enabling a more comprehensive identification of the most relevant features. To address the class imbalance, SMOTE oversampling was applied before this step to balance the minority (PD) and majority (healthy) classes at a 1:1 ratio.

To leverage the complementary strengths of these models, a weighted averaging approach was employed to consolidate the feature importance scores. This method integrated insights from all models, ensuring a balanced and comprehensive feature selection that optimally reflected the data's predictive potential.

A coarse-to-fine search strategy was implemented to determine the optimal feature importance threshold. Initially, a coarse search identified a broad threshold range, followed by a finer search within this range to precisely pinpoint the threshold that maximizes model performance. This approach was grounded in the observation that prediction performance initially improved as overfitting was mitigated and later declined as too much information was discarded.

This two-stage search strategy enhanced efficiency by reducing the number of features appropriately to ensure predictive accuracy. The resulting optimized feature set not only improved model generalizability but also enhanced interpretability.

3.4 Adaptive Ensemble Learning for PD Detection

With the resampled and selected features, we then built our ensemble learning model. PD exhibits significant clinical heterogeneity, resulting in variable performance of classification algorithms across different patient populations. To address this challenge, we proposed an adaptive ensemble learning approach that dynamically integrated five distinct classifiers: SVM, decision trees, logistic regression, linear discriminant analysis (LDA), and k-nearest neighbors (KNN). The adaptive aspect of this method lay in its ability to fine-tune and combine classifiers based on their complementary strengths, ensuring optimal performance across diverse populations.

The five classifiers were selected for their complementary strengths in handling different data characteristics: SVM is particularly effective in handling high-dimensional spaces and non-linear boundaries, while decision trees excel in interpretability and adaptability to non-parametric data. Logistic regression provides simplicity and robustness for linearly separable data, LDA is well-suited for modeling class separability under Gaussian assumptions, and KNN captures local patterns in the data without imposing strong parametric assumptions. By adaptively leveraging these strengths through a voting-based ensemble, the classification accuracy was improved.

Before classification, z-score standardization was applied to normalize feature scales.To maximize the potential of the ensemble, a grid search framework was employed to adaptively fine-tune the hyperparameters of each classifier. Considering the class imbalance, the F1 score was priortized during the adaptive hyperparameter tuning to prevent bias towards majority classes. The detailed hyperparameters for adaptive fine-tuning were presented in Table 2.

The adaptive nature of our hard-voting ensemble stems from the optimization of its individual components. The built-in grid search process tailors each classifier to the unique characteristics of

the dataset, creating a set of highly specialized experts. This systematic specialization allows the ensemble to collectively and reliably handle the varying clinical manifestations of Parkinson's disease.

4 Results and Discussion

To evaluate the effectiveness of the proposed methods, we conducted a series of experiments to validate the performance of the feature selection strategies and ensemble models. First, we presented the results of correlation analysis to identify redundancies within the data. Next, we analyzed the feature importance and selection outcomes. Additionally, we performed an ablation study to assess the impact of each stage in the sequential feature selection process. Finally, we compared the performance of the adaptive voting ensemble with various base learners and popular ensemble methods.

4.1 Feature Importance of Different Models

To support refined feature selection through integrated model-driven analysis, we first analyzed the feature importance of four models: SVM, random forests, AdaBoost, and XGBoost. Figure 3 shows the results. The analysis revealed both similarities and differences in how features were selected by each model.

Certain features consistently ranked as critical predictors across all models, such as the average pitch angle during the loading phase (LoadingPitchMean), the percentage of loading duration relative to the total gait cycle (LoadingDurationPercentInGc), and the coefficient of variation of loading duration (LoadingDurationCV). These features highlight their importance to the task. Temporal and spatial metrics also stand out as dominant factors, reflecting their ability to effectively capture underlying patterns.

Despite these commonalities, the models differ in how they prioritize features. SVM focuses on a smaller subset of features, particularly those related to the loading and pushing phases, along with stride length and step height. In contrast, the three tree-based ensemble methods assign importance to a wider range of features, including those related to the swing and mid-stance phases. XGBoost uniquely emphasizes the variation in pitch velocity during the mid-stance phase (midFlatfootVelCv), which is less significant in other models. This suggests that XGBoost excels at identifying complex feature interactions.

The integrated results, presented in Figure 4, summarize the feature importance rankings from all models. Key features, such as LoadingPitchMean, LoadingDurationPercentInGc, and LoadingDurationCV, consistently rank highly. These features are confirmed as important predictors, reflecting their significance in gait-phase-specific dynamics.

Some features, like midFlatfootVelCv emphasized by XGBoost, hold moderate importance in the combined results. This highlights their unique but valuable role in capturing specific patterns. Spatio-temporal metrics dominate the rankings, including features from the loading, swing, and mid-stance phases, which are effective at identifying underlying trends.

These findings highlight the complementary strengths of the models in identifying important features. Combining the feature importance results from multiple models provides a more comprehensive understanding and improves the overall feature selection process.

4.2 Coarse-to-fine Threshold Optimization and Feature Selection

To determine the optimal number of features, we first performed a coarse search by dividing the range from 0 to the maximum feature importance into 50 equal intervals. Using five-fold cross-validation with the XGBoost model (which achieved the highest F1 score among the four models used for feature selection) on the training set, we evaluated model performance at each threshold. This approach allowed us to quickly narrow down the potential optimal threshold range, with the coarse search identifying a preliminary threshold of 0.0095. This step was essential for establishing a general range for further refinement.

Next, we focused on the interval around the preliminary threshold, narrowing it down to 0.006–0.011. We then conducted a fine search, dividing this range into 50 equal intervals. This fine search precisely

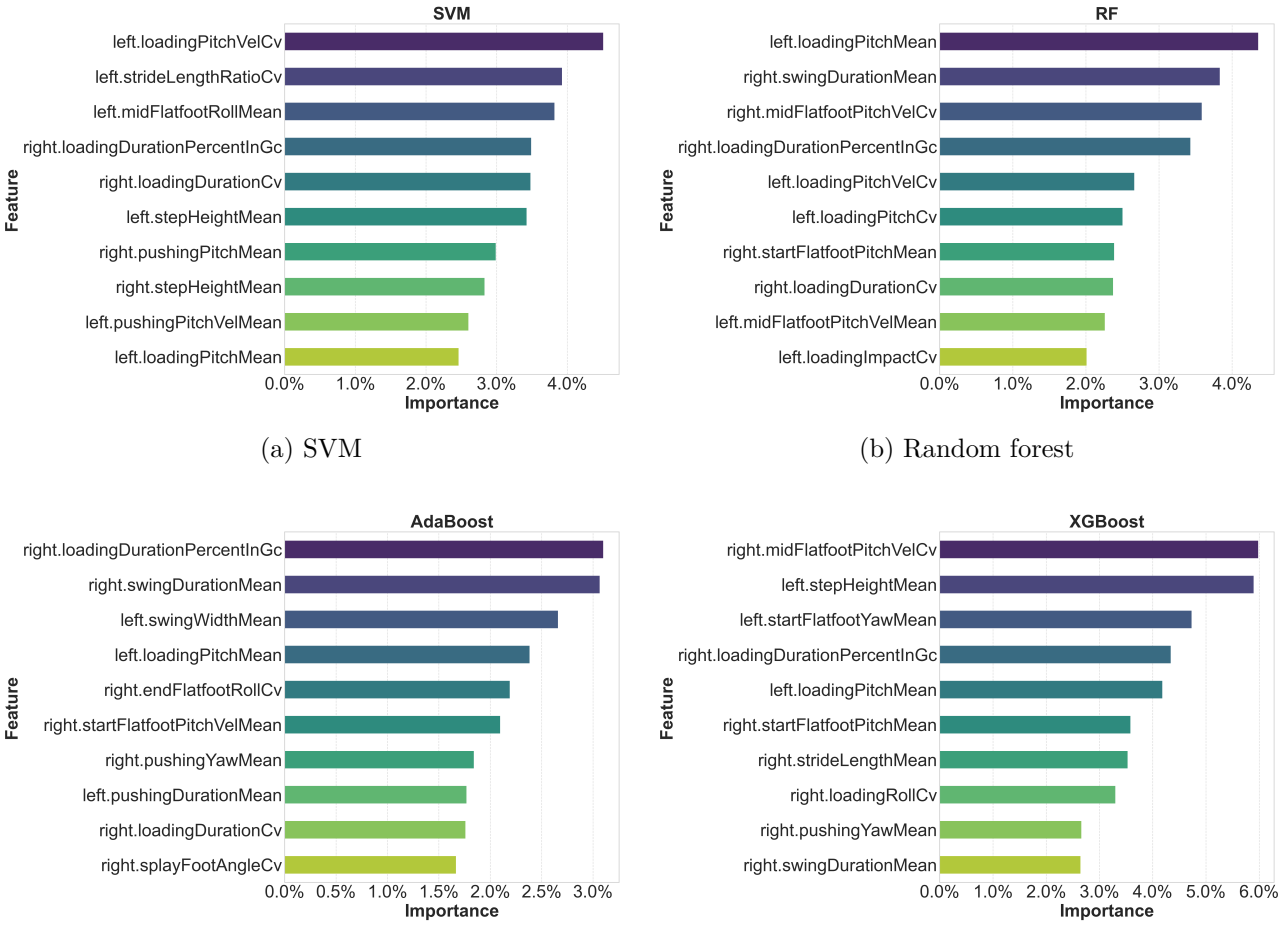

(a) SVM (b) Random forest

(c) AdaBoost (d) XGBoost

Figure 3: Top 10 important features of four different models.

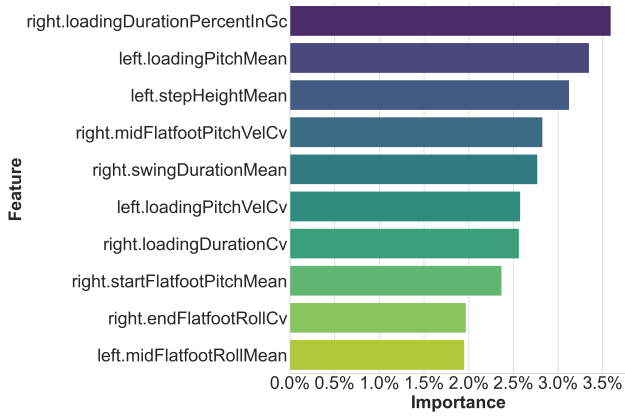

Figure 4: Top 10 important features after integrating the results of four models.

identified the feature importance threshold that yielded the best model performance. The final optimal threshold was determined to be 0.00892. The coarse-to-fine search process is illustrated in Figure 5. Each point in the figure represents the mean F1 score ± standard deviation over five repeated runs.

Based on this threshold, we selected 41 features, as shown in Table 3. These features were subsequently examined from clinical and biomechanical perspectives and discussed with collaborating clinicians.

The selected gait features demonstrate strong clinical relevance, capturing the cardinal motor symptoms of Parkinson's disease (PD), including bradykinesia, rigidity, and postural instability.

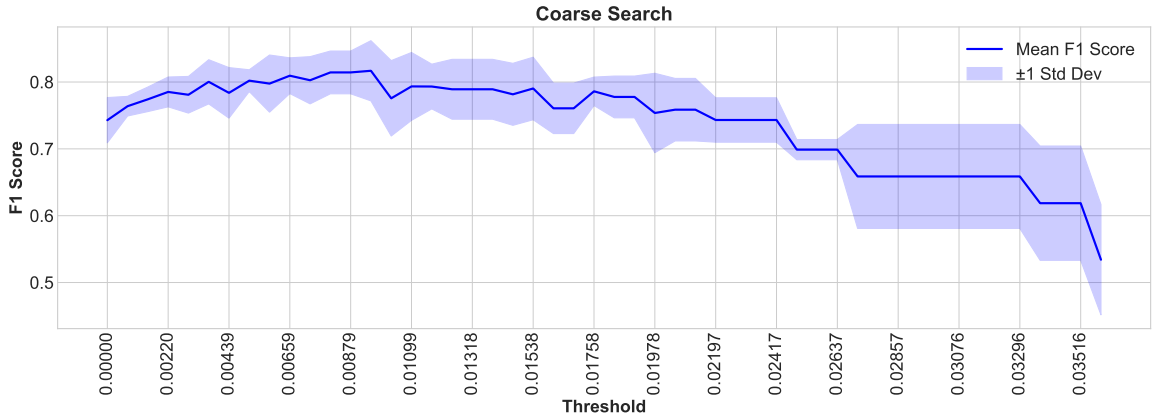

(a) Coarse search for the optimized threshold of feature importance.

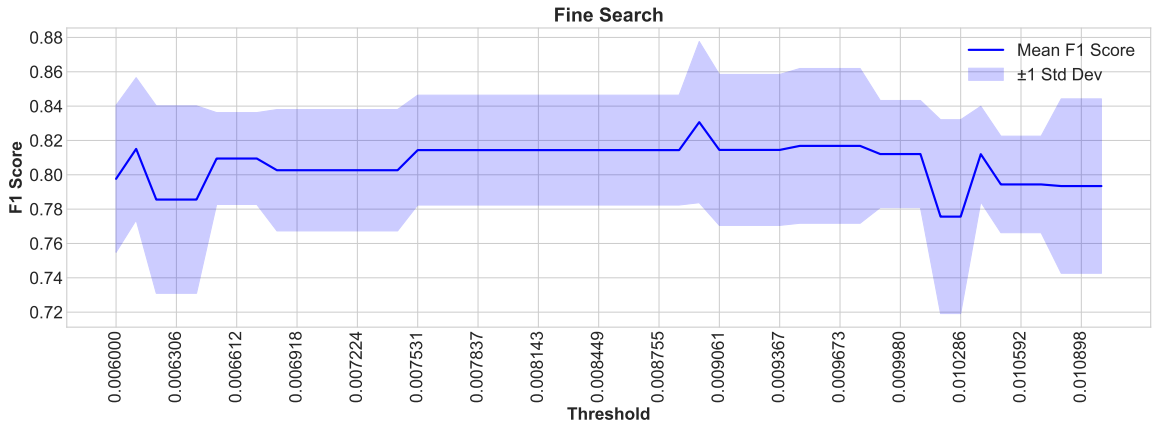

(b) Fine search for the optimized threshold of feature importance.

Figure 5: Coarse-to-fine Threshold Optimization.

Temporal-spatial parameters, such as stride length and swing duration, directly quantify the prominent PD symptom of gait bradykinesia. High coefficients of variation (Cv), which recur across multiple parameters, serve as key indicators of impaired gait rhythmicity and increased variability. Such instability is a well-documented marker of postural control deficits and is strongly associated with an elevated risk of falls in PD patients.

Analyzing distinct gait cycle phases—loading, flatfoot, push-off, and swing—provides a more detailed understanding of motor deficits. For example, push-off phase parameters, such as pushingPitchVelMean, are critical for assessing the reduced propulsion force common in PD, which contributes to the characteristic shuffling gait. Similarly, features from the loading and flatfoot phases (e.g., loadingDurationPercentInGc) reflect impaired anticipatory postural adjustments and static balance control. These fine-grained metrics go beyond basic temporal-spatial measurements to offer deeper insight into biomechanical and motor control abnormalities.

The inclusion of multiple kinematic parameters (e.g., pitch, roll, and yaw angles and velocities) further enhances the clinical utility of the feature set. These measures quantify joint rigidity and reduced range of motion—hallmark signs of PD. For instance, splayFootAngle and swingWidth can capture compensatory strategies patients use to maintain balance, while variations in pitch and roll velocities reflect stiff, uncoordinated movements. Subtle changes and increasing variability in kinematic data may also serve as potential early indicators of freezing of gait (pre-FoG) events.

In summary, the selected features encompass a comprehensive set of temporal-spatial, kinematic, and variability metrics, capturing critical aspects of gait dynamics and the complex interactions between different gait phases. This multidimensional feature set provides a robust foundation for objective assessment of PD gait impairments, supporting both clinical diagnosis and technology-based monitoring.

Table 3: Final selected 41 gait parameters

No.	Feature	Type	No.	Feature	Type
		Loading Phase			
1	right.loadingDurationPercentInGc	Temporal	2	right.loadingDurationCv	Temporal
3	left.loadingPitchMean	Kinematic	4	left.loadingPitchVelCv	Kinematic
5	right.loadingRollCv	Kinematic	6	left.loadingImpactCv	Kinetic
		Flatfoot Phase			
7	right.startFlatfootPitchMean	Kinematic	8	left.startFlatfootPitchCv	Kinematic
9	right.startFlatfootPitchVelMean	Kinematic	10	left.startFlatfootPitchVelCv	Kinematic
11	left.startFlatfootYawMean	Kinematic	12	left.midFlatfootPitchVelMean	Kinematic
13	right.midFlatfootPitchVelCv	Kinematic	14	left.midFlatfootRollMean	Kinematic
15	right.midFlatfootYawMean	Kinematic	16	left.endFlatfootPitchCv	Kinematic
17	right.endFlatfootPitchCv	Kinematic	18	left.endFlatfootPitchVelCv	Kinematic
19	right.endFlatfootRollCv	Kinematic	20	left.endFlatfootRollCv	Kinematic
		Push-off Phase			
21	left.pushingDurationMean	Temporal	22	left.pushingDurationCv	Temporal
23	left.pushingPitchVelMean	Kinematic	24	right.pushingPitchMean	Kinematic
25	right.pushingYawMean	Kinematic			
		Swing Phase			
26	left.stepHeightMean	Spatial	27	right.stepHeightMean	Spatial
28	left.swingWidthMean	Spatial	29	right.swingWidthCv	Spatial
30	right.swingDurationMean	Temporal	31	right.swingDurationCv	Temporal
32	left.splayFootAngleMean	Kinematic	33	right.splayFootAngleMean	Kinematic
34	left.maxRollVelCv	Kinematic	35	right.maxRollVelMean	Kinematic
		Full Cycle / Cross-Phase			
36	left.strideLengthMean	Spatial	37	right.strideLengthMean	Spatial
38	left.strideLengthRatioCv	Spatial	39	right.stanceDurationPercentInGc	Temporal
40	right.loadingDurationCv	Temporal	41	left.rollScaleMean	Kinematic

4.3 Ablation Study for Sequential Feature Selection Strategy

To evaluate the effects of the sequential feature selection strategy, we conducted an ablation study to assess each stage of the sequential method. Table 4 presents the comparative results. The findings indicate that the sequential approach achieves the best balance between feature reduction and classification performance. Although using all features yields the highest accuracy and AUC, it also results in the longest training time. In contrast, the filtering and integration-based methods reduce the feature set but cause a noticeable decline in performance, particularly in accuracy and F1 score.

The sequential feature selection method achieves competitive accuracy and F1 score while significantly reducing both the number of features and the training time compared to using the full feature set. These results highlight the effectiveness of the sequential approach in improving model efficiency without substantially compromising performance.

Table 4: Comparative experimental results for different feature selection strategies

Feature Selection	# of Selected Features	AUC	F1 Score	Classification Model Training Time (s)
All features	164	0.9147±0.0298	0.9103±0.0438	12.16
Only Filtering	95	0.8856±0.0316	0.8784±0.0542	7.30
Only Integrating	65	0.8894±0.0254	0.8837±0.0421	8.60
Sequential Methods	41	0.9053±0.0095	0.8958±0.0120	8.22

4.4 Comparison between different classification models

To validate the effectiveness of the proposed adaptive voting ensemble model, we compared its performance against five base learners and three popular ensemble methods: random forest, gradient boosting decision trees (GBDT), and light gradient boosting machine (LightGBM). In addition, we considered a UPDRS-based clinical baseline: previous studies have reported AUC values ranging from 0.59 to 0.69 [25] for PD identification using MDS-UPDRS scores. The results, summarized in Table 5, are reported as mean values with standard deviations estimated via bootstrap resampling ($n = 1000$).

The five base learners exhibited varying performance levels. KNN and SVM achieved the highest F1 scores and AUC values, demonstrating strong predictive power in distinguishing Parkinson's disease (PD) patients from healthy controls. In contrast, logistic regression and decision tree underperformed, highlighting their limitations in capturing the diverse characteristics of PD patients.

Among the ensemble methods, all four strategies improved performance compared to individual models. Notably, the proposed adaptive voting ensemble outperformed the other three ensemble methods, achieving the highest F1 score (0.8959) and AUC (0.9055). These results underscore the advantage of combining multiple classifiers with diverse structures, enabling the model to effectively leverage their strengths to capture the heterogeneity within PD patient subsets.

To further mitigate class imbalance, we also evaluated the performance with SMOTE oversampling. The adaptive voting ensemble achieved comparable results (F1 score 0.8921, AUC 0.9028), confirming robustness.

Given the scale of the data, we primarily compared our results with those of Zhang et al. [33]. While their study achieved an AUC score of 0.8558 using the mPower dataset collected via smartphones, our approach achieved a higher AUC score of 0.9055 using data collected from IMUs attached to insoles. Unlike smartphone sensors, which are sensitive to varying positioning and user-related motion artifacts, foot-mounted sensors provide more accurate and consistent gait data. This improved data quality contributes to better gait analysis, enabling more precise detection of PD.

5 Conclusions

This study proposed an ensemble learning approach for the early diagnosis of PD based on gait analysis. We constructed a novel dataset comprising over 3,000 samples from both PD patients and

Table 5: Comparative experimental results for different classification models

Algorithm	F1 Score	AUC
Logistic Regression	0.8015 ± 0.0124	0.8139 ± 0.0105
SVM	0.8584 ± 0.0111	0.8739 ± 0.0088
Decision Tree	0.7749 ± 0.0134	0.7972 ± 0.0107
KNN	0.8611 ± 0.0100	0.8648 ± 0.0091
LDA	0.8297 ± 0.0120	0.8387 ± 0.0103
Random Forest	0.8749 ± 0.0098	0.8870 ± 0.0080
GBDT	0.8855 ± 0.0095	0.8961 ± 0.0078
LightGBM	0.8903 ± 0.0092	0.9000 ± 0.0077
Voting Ensemble (Ours)	**0.8958 ± 0.0120**	**0.9053 ± 0.0095**

healthy controls, utilizing 6-axis IMUs to capture 164 gait features. To address the challenge of high-dimensional data, we introduced a sequential feature selection strategy that combined filtering and embedded methods, effectively reducing the feature set to 41 key parameters.

The adaptive voting ensemble model developed in this study, which integrated five different classifiers, achieved an F1 score of 89.58% and an AUC of 90.53%. These results demonstrated its strong ability to distinguish PD patients from healthy individuals. The model not only improved diagnostic performance but also provided valuable insights into the gait characteristics associated with PD, offering a robust and interpretable tool for early diagnosis.

Future work will address both methodological and practical challenges. On the methodological side, we plan to expand our dataset to improve class balance and incorporate detailed clinical metadata for more comprehensive monitoring and management. We will also enhance our model's adaptability by exploring dynamic weighted voting strategies that can better handle varying clinical presentations. To validate our approach, we will perform external validation on both public datasets (e.g., mPower, Daphnet) and newly collected clinical cohorts using a standardized feature-extraction pipeline. Furthermore, we aim to leverage richer sequential gait data to develop interpretable deep temporal models that can capture fine-grained temporal patterns while maintaining clinical interpretability, ultimately supporting earlier interventions and improved outcomes for individuals with PD.

On the practical side, future work will explore a robust edge-cloud collaboration framework. This involves deploying lightweight models on edge devices for real-time feedback and securely transmitting data to the cloud for comprehensive, long-term monitoring. This synergy will enable continuous disease progression monitoring while ensuring full data privacy and compliance.

Funding

The study was funded by the National Key Research and Development Program of China (grant number: 2024YFC3606700).

Author contributions

Zheng Zhimin, Gong Kaidi, and Gong Chen have equally contributed to this manuscript and are to be recognized as co-first authors.

Conflict of interest

The authors declare no conflict of interest.

Appendix: Gait Parameters in Our Dataset

To provide a comprehensive overview of our work, we present the 164 gait parameters included in our dataset in Tables 6–10, organized by gait phase. For brevity, only half of the features are displayed here; in the complete dataset, each feature is further distinguished by left and right foot.

Table 6: Gait parameters characterizing the full gait cycle or cross-phase dynamics

No.	Feature	Type	No.	Feature	Type
1	cycleDurationCv	Temporal	2	stanceDurationMean	Temporal
3	stanceDurationCv	Temporal	4	stanceDurationPercentInGc	Temporal
5	strideLengthMean	Spatial	6	strideLengthCv	Spatial
7	strideLengthRatioMean	Spatial	8	strideLengthRatioCv	Spatial
9	pathLength3dMean	Spatial	10	pathLength3dCv	Spatial
11	splayFootAngleMean	Spatial	12	splayFootAngleCv	Spatial
13	maxRollVelMean	Kinematic	14	maxRollVelCv	Kinematic
15	rollScaleMean	Kinematic	16	rollScaleCv	Kinematic
17	yawScaleMean	Kinematic	18	yawScaleCv	Kinematic
19	supportStabilityMean	Kinetic	20	supportStabilityCv	Kinetic

Table 7: Gait parameters characterizing the loading phase

No.	Feature	Type	No.	Feature	Type
1	loadingDurationMean	Temporal	2	loadingDurationCv	Temporal
3	loadingDurationPercentInGc	Temporal	4	loadingPitchMean	Kinematic
5	loadingPitchCv	Kinematic	6	loadingRollMean	Kinematic
7	loadingRollCv	Kinematic	8	loadingYawMean	Kinematic
9	loadingYawCv	Kinematic	10	loadingPitchVelMean	Kinematic
11	loadingPitchVelCv	Kinematic	12	loadingImpactMean	Kinetic
13	loadingImpactCv	Kinetic			

Table 8: Gait parameters characterizing the flatfoot phase

No.	Feature	Type	No.	Feature	Type
1	flatfootDurationMean	Temporal	2	flatfootDurationCv	Temporal
3	flatfootDurationPercentInGc	Temporal	4	startFlatfootPitchMean	Kinematic
5	startFlatfootPitchCv	Kinematic	6	startFlatfootRollMean	Kinematic
7	startFlatfootRollCv	Kinematic	8	startFlatfootYawMean	Kinematic
9	startFlatfootYawCv	Kinematic	10	startFlatfootPitchVelMean	Kinematic
11	startFlatfootPitchVelCv	Kinematic	12	midFlatfootPitchMean	Kinematic
13	midFlatfootPitchCv	Kinematic	14	midFlatfootRollMean	Kinematic
15	midFlatfootRollCv	Kinematic	16	midFlatfootYawMean	Kinematic
17	midFlatfootYawCv	Kinematic	18	midFlatfootPitchVelMean	Kinematic
19	midFlatfootPitchVelCv	Kinematic	20	endFlatfootPitchMean	Kinematic
21	endFlatfootPitchCv	Kinematic	22	endFlatfootRollMean	Kinematic
23	endFlatfootRollCv	Kinematic	24	endFlatfootYawMean	Kinematic
25	endFlatfootYawCv	Kinematic	26	endFlatfootPitchVelMean	Kinematic
27	endFlatfootPitchVelCv	Kinematic			

Table 9: Gait parameters characterizing the pushing phase

No.	Feature	Type	No.	Feature	Type
1	pushingDurationMean	Temporal	2	pushingDurationCv	Temporal
3	pushingDurationPercentInGc	Temporal	4	pushingPitchMean	Kinematic
5	pushingPitchCv	Kinematic	6	pushingRollMean	Kinematic
7	pushingRollCv	Kinematic	8	pushingYawMean	Kinematic
9	pushingYawCv	Kinematic	10	pushingPitchVelMean	Kinematic
11	pushingPitchVelCv	Kinematic			

Table 10: Gait parameters characterizing the swing phase

No.	Feature	Type	No.	Feature	Type
1	swingDurationMean	Temporal	2	swingDurationCv	Temporal
3	swingDurationPercentInGc	Temporal	4	maxSwingVelMean	Kinematic
5	maxSwingVelCv	Kinematic	6	swingWidthMean	Spatial
7	swingWidthCv	Spatial	8	stepHeightMean	Spatial
9	stepHeightCv	Spatial	10	maxPitchVelMean	Kinematic
11	maxPitchVelCv	Kinematic			

References

[1] Balakrishnan, A.; Medikonda, J.; Namboothiri, P.K. (2022). Role of wearable sensors with machine learning approaches in gait analysis for Parkinson's disease assessment: a review, *Engineered Science*, 19, 5–19, 2022.

[2] Bayés, À.; Samá, A.; Prats, A.; Pérez-López, C.; Crespo-Maraver, M.; Moreno, J.M.; Alcaine, S.; Rodriguez-Molinero, A.; Mestre, B.; Quispe, P. (2018). A "HOLTER" for Parkinson's disease: Validation of the ability to detect on-off states using the REMPARK system, *Gait & posture*, 59, 1–6, 2018.

[3] Bhidayasiri, R.; Tarsy, D. (2012). Parkinson's disease: Hoehn and Yahr scale, *Movement disorders: a video atlas*, 4–5, 2012.

[4] Bloem, B.R.; Okun, M.S.; Klein, C. (2021). Parkinson's disease, *The Lancet*, 397(10291), 2284–2303, 2021.

[5] Caramia, C.; Torricelli, D.; Schmid, M.; Munoz-Gonzalez, A.; Gonzalez-Vargas, J.; Grandas, F.; Pons, J.L. (2018). IMU-based classification of Parkinson's disease from gait: A sensitivity analysis on sensor location and feature selection, *IEEE journal of biomedical and health informatics*, 22(6), 1765–1774, 2018.

[6] Chen, B.R.; Patel, S.; Buckley, T.; Rednic, R.; McClure, D.J.; Shih, L.; Tarsy, D.; Welsh, M.; Bonato, P. (2011). A web-based system for home monitoring of patients with Parkinson's disease using wearable sensors, *IEEE Trans Biomed Eng*, 58(3), 831–836, 2011.

[7] Crenna, P.; Carpinella, I.; Rabuffetti, M.; Calabrese, E.; Mazzoleni, P.; Nemni, R.; Ferrarin, M. (2007). The association between impaired turning and normal straight walking in Parkinson's disease, *Gait & posture*, 26(2), 172–178, 2007.

[8] Das, S.; Amoedo, B.; De la Torre, F.; Hodgins, J. (2012). Detecting Parkinsons' symptoms in uncontrolled home environments: A multiple instance learning approach, *2012 Annual International Conference of the IEEE Engineering in Medicine and Biology Society*, 3688–3691, 2012.

[9] Dijkstra, B.; Kamsma, Y.P.; Zijlstra, W. (2010). Detection of gait and postures using a miniaturized triaxial accelerometer-based system: accuracy in patients with mild to moderate Parkinson's disease, *Arch Phys Med Rehabil*, 91(8), 1272–1277, 2010.

[10] Funayama, M.; Nishioka, K.; Li, Y.; Hattori, N. (2023). Molecular genetics of Parkinson's disease: Contributions and global trends, *Journal of human genetics*, 68(3), 125–130, 2023.

[11] Galna, B.; Lord, S.; Burn, D.J.; Rochester, L. (2015). Progression of gait dysfunction in incident Parkinson's disease: impact of medication and phenotype, *Movement Disorders*, 30(3), 359–367, 2015.

[12] Giladi, N.; Shabtai, H.; Simon, E.S.; Biran, S.; Tal, J.; Korczyn, A.D. (2000). Construction of freezing of gait questionnaire for patients with Parkinsonism, *Parkinsonism & related disorders*, 6(3), 165–170, 2000.

[13] Goetz, C.G.; Tilley, B.C.; Shaftman, S.R.; Stebbins, G.T.; Fahn, S.; Martinez-Martin, P.; Poewe, W.; Sampaio, C.; Stern, M.B.; Dodel, R.; et al. (2008). Movement Disorder Society-sponsored revision of the Unified Parkinson's Disease Rating Scale (MDS-UPDRS): scale presentation and clinimetric testing results, *Movement disorders: official journal of the Movement Disorder Society*, 23(15), 2129–2170, 2008.

[14] Kharb, A.; Saini, V.; Jain, Y.K.; Dhiman, S. (2011). A review of gait cycle and its parameters, *IJCEM International Journal of Computational Engineering & Management*, 13(01), 2011.

[15] Maertens, W.; Vangeyte, J.; Baert, J.; Jantuan, A.; Mertens, K.C.; De Campeneere, S.; Pluk, A.; Opsomer, G.; Van Weyenberg, S.; Van Nuffel, A. (2011). Development of a real time cow gait tracking and analysing tool to assess lameness using a pressure sensitive walkway: The GAITWISE system, *Biosystems Engineering*, 110(1), 29–39, 2011.

[16] Martinez, C.; Rodriguez, S.; Gomez, L. (2021). Validation of a smartphone-based gait analysis tool for Parkinson's disease monitoring, *Parkinsonism & Related Disorders*, 92, 45–52, 2021.

[17] Meng, L.; Pang, J.; Yang, Y.F.; Chen, L.; Xu, R.; Ming, D. (2023). Inertial-based gait metrics during turning improve the detection of early-stage parkinson's disease patients, *IEEE Transactions on Neural Systems and Rehabilitation Engineering*, 31, 1472–1482, 2023.

[18] Mirelman, A.; Ben Or Frank, M.; Melamed, M.; Granovsky, L.; Nieuwboer, A.; Rochester, L.; Del Din, S.; Avanzino, L.; Pelosin, E.; Bloem, B.R.; et al. (2021). Detecting Sensitive Mobility Features for Parkinson's Disease Stages Via Machine Learning, *Mov Disord*, 36(9), 2144–2155, 2021.

[19] Movement Disorder Society Task Force on Rating Scales for Parkinson's Disease. (2003). The unified Parkinson's disease rating scale (UPDRS): status and recommendations, *Movement Disorders*, 18(7), 738–750, 2003.

[20] Park, H.; Shin, S.; Youm, C.; Cheon, S.M.; Lee, M.; Noh, B. (2021). Classification of Parkinson's disease with freezing of gait based on 360 degrees turning analysis using 36 kinematic features, *Journal of NeuroEngineering and Rehabilitation*, 18(1), 177, 2021.

[21] Pastorino, M.; Cancela, J.; Arredondo, M.T.; Pansera, M.; Pastor-Sanz, L.; Villagra, F.; Pastor, M.A.; Martin, J.A. (2011). Assessment of bradykinesia in Parkinson's disease patients through a multi-parametric system, *2011 Annual International Conference of the IEEE Engineering in Medicine and Biology Society*, 1810–1813, 2011.

[22] Pfister, A.; West, A.M.; Bronner, S.; Noah, J.A. (2014). Comparative abilities of Microsoft Kinect and Vicon 3D motion capture for gait analysis, *Journal of medical engineering & technology*, 38(5), 274–280, 2014.

[23] Pistacchi, M.; Gioulis, M.; Sanson, F.; De Giovannini, E.; Filippi, G.; Rossetto, F.; Marsala, S.Z. (2017). Gait analysis and clinical correlations in early Parkinson's disease, *Functional neurology*, 32(1), 28, 2017.

[24] Rehman, R.Z.U.; Del Din, S.; Guan, Y.; Yarnall, A.J.; Shi, J.Q.; Rochester, L. (2019). Selecting clinically relevant gait characteristics for classification of early Parkinson's disease: a comprehensive machine learning approach, *Scientific reports*, 9(1), 17269, 2019.

[25] Rom H, Peleg O, Rom Y, Mirelman A, Blumrosen G, Maidan I. Remote clinical decision support tool for Parkinson's disease assessment using a novel approach that combines AI and clinical knowledge. (2025) *BMC Medical Informatics and Decisison Making.* 25(1), 294, 2025

[26] Shi, B.; Tay, A.; Au, W.L.; Tan, D.M.L.; Chia, N.S.Y.; Yen, S.C. (2022). Detection of Freezing of Gait Using Convolutional Neural Networks and Data From Lower Limb Motion Sensors, *IEEE Transactions on Biomedical Engineering*, 69(7), 2256–2267, 2022.

[27] Smith, J.; Johnson, E.; Williams, R. (2022). Predicting motor complications in Parkinson's disease using machine learning and gait analysis, *Journal of Neural Engineering*, 19(3), 036021, 2022.

[28] Ullrich, M.; Roth, N.; Kuderle, A.; Richer, R.; Gladow, T.; Gassner, H.; Marxreiter, F.; Klucken, J.; Eskofier, B.M.; Kluge, F. (2022). Fall risk prediction in Parkinson's disease using real-world inertial sensor gait data, *IEEE journal of biomedical and health informatics*, 27(1), 319–328, 2022.

[29] Vallabhajosula, S.; Buckley, T.A.; Tillman, M.D.; Hass, C.J. (2013). Age and Parkinson's disease related kinematic alterations during multi-directional gait initiation, *Gait Posture*, 37(2), 280–286, 2013.

[30] Wang, Y.; Liu, X.; Zhao, W. (2022). Deep learning approaches for gait pattern recognition in neurodegenerative diseases, *Artificial Intelligence in Medicine*, 120, 102256, 2022.

[31] Wang, Xiaotian and Xu, Xuanhang and Zhao, Zhifu and Li, Fu and Qi, Fei and Liang, Shuo. (2025). VGRF Signal-Based Gait Analysis for Parkinson's Disease Detection: A Multi-Scale Directed Graph Neural Network Approach, *IEEE Journal of Biomedical and Health Informatics*, 1–13, 2025.

[32] Yang, Y.F.; Chen, L.; Pang, J.; Huang, X.Y.; Meng, L.; Ming, D. (2022). Validation of a spatiotemporal gait model using inertial measurement units for early-stage Parkinson's disease detection during turns, *IEEE Transactions on Biomedical Engineering*, 69(12), 3591–3600, 2022.

[33] Zhang, H.; Deng, K.; Li, H.; Albin, R.; Guan, Y. (2020). Deep Learning Identifies Digital Biomarkers for Self-Reported Parkinson's Disease, *Patterns*, 1(3), 100042, 2020.

Journal's webpage: http://univagora.ro/jour/index.php/ijccc/

This journal is a member of, and subscribes to the principles of,
the Committee on Publication Ethics (COPE).
https://publicationethics.org/members/international-journal-computers-communications-and-control

Cite this paper as:

Zheng, Z.; Gong, K.; Gong, C.; Zhang, L.; Meng, L.; He, F.; (2026). Sequential Feature Selection and Adaptive Ensemble Classification for Parkinson's Disease Detection, *International Journal of Computers Communications & Control*, 21(5), 7202, 2026.

https://doi.org/10.15837/ijccc.2026.5.7202